View metadata, citation and similar papers at core.ac.uk

brought to you by CORE

provided by IntechOpen

We are IntechOpen, the world's leading publisher of Open Access books Built by scientists, for scientists

4,800
Open access books available

122,000
International authors and editors

135M
Downloads

Our authors are among the

154
Countries delivered to

TOP 1%
most cited scientists

12.2%
Contributors from top 500 universities

CLARIVATE ANALYTICS BOOK CITATION INDEX INDEXED

WEB OF SCIENCE™

Selection of our books indexed in the Book Citation Index in Web of Science™ Core Collection (BKCI)

Interested in publishing with us?
Contact book.department@intechopen.com

Numbers displayed above are based on latest data collected.
For more information visit www.intechopen.com

8

Electrical Processes in Polycrystalline $BiFeO_3$ Film

Yawei Li[1], Zhigao Hu[1] and Junhao Chu[1,2]
[1]*Key Laboratory of Polar Materials and Devices, Ministry of Education, Department of Electronic Engineering, East China Normal University, Shanghai*
[2]*National Laboratory for Infrared Physics, Shanghai Institute of Technical Physics, Chinese Academy of Sciences, Shanghai*
People's Republic China

1. Introduction

As an oxide with perovskite structure, Bismuth ferrite ($BiFeO_3$, BFO) has been studied from 1970s (Teague, et al. 1970; Kaczmarek, et al. 1975). The structure and magnetic properties of BFO were confirmed before 1970s. As reported, the crystal structure of BFO is perovskite with rhombohedral distortion and the space group is R3c. BFO is G-type antiferromagnetic. It was controversial about whether BFO was ferroelectrics until the hysteresis loop of single crystal BFO was measured in 1970 (Teague, et al. 1970). According to Teague's results, the single crystal BFO was anisotropy. The remnant polarizations (P_r) along the (100) and (111) direction were 3.5μC/cm² and 6.1μC/cm² at the temperature of liquid nitrogen, respectively. However, because of the higher leakage current in the bulk BFO, it was difficult to measure the ferroelectric properties of BFO at room temperature. The problem of higher leakage blocks not only the studies of the electrical properties of BFO, but also the application of BFO in electrical devices. In 2003, the epitaxial BFO films with higher electrical resistivity and higher remnant polarization was fabricated by pulsed laser deposition (PLD) method (J. Wang, 2003). The value of P_r of the epitaxial BFO films is about 50μC/cm². This value is larger than that of the traditional ferroelectrics such as $Pb(Zr,Ti)O_3$ (PZT), $BaTiO_3$ (BTO). If the BFO film with larger P_r can be used in ferroelectric memory (FeRAM), the size of the storage cell can be reduced and the storage density can be increased (Maruyama, 2007). More studies on BFO films are carried out (Eerenstein, 2005; Zavaliche, 2005; Singh, 2007; Hauser, 2008; Liu, 2008; Yang, 2008). Even though the leakage mechanism in epitaxial BFO film has been studied (Pabst, 2007), the higher leakage current is still an obstacle for the study and application of polycrystalline BFO films. Compared to the epitaxial BFO films grown on perovskite structure substrate, the applications of polycrystalline BFO on silicon wafer are broader in the field of microelectronic devices. In this chapter, polycrystalline BFO films are fabricated by different physical and chemical methods on buffered silicon and perovskite structure substrate. The structural and electrical properties of these polycrystalline BFO films are investigated.

2. Experiments

Considering the universality of our conclusion for different polycrystalline BFO films, the samples studied in this work are fabricated by two different methods, PLD and chemical solution deposition (CSD) methods. The former is a typical physical method of film deposition. The later is a chemical method. At the same time, different materials are used as substrate. For the samples prepared by PLD, n-type silicon covered by a layer of (La,Sr)CoO_3 (LSCO) is used as substrate. The layer of LSCO acts as bufferlayer for the growth of BFO and bottom electrode for the electrical measurement. For the samples prepared by CSD, the single crystal $SrTiO_3$ (STO) covered by $LaNiO_3$ (LNO) is used as substrate.

2.1 The fabrications of BFO films by PLD method

For the preparation of polycrystalline BFO films by PLD method, single-side polished silicon wafer is used as substrate. Before the deposition of BFO film, a layer of LSCO is deposited on the surface of silicon wafer by PLD. The component of the LSCO target is $(La_{0.5}Sr_{0.5})CoO_3$. The component of BFO target is $Bi_{1.05}FeO_3$. The excess bismuth is used to compensate the evaporation of bismuth at higher temperature during the growth of BFO films. The depositions of LSCO and BFO are carried out in a vacuum chamber with background pressure lower than 10^{-4} Pa. A KrF excimer laser with the wavelength of 248 nm is used for the deposition. During the deposition of LSCO layer, the oxygen pressure in the chamber is about 25 Pa. The temperature of the silicon wafer is 650°C (Li, 2009). Details about the deposition conditions are listed in table 1. The deposition of LSCO layer is carried out for 20 minutes. After the deposition, the oxygen pressure in the chamber increased to 50 Pa and maintained for 30 min. The thickness of the LSCO layer is about 200 nm obtained from the scanning electronic microscope.

Target	LSCO	BFO
Frequency of pulse	5Hz	3Hz
Oxygen pressure	25Pa	3Pa
Substrate temperature	650°C	700°C
Deposition time	20min	90min
Holding temperature	650°C	495°C
Holding oxygen pressure	50 Pa	3Pa/1.01×10^5 Pa
Holding time	30min	30min

Table 1. The deposition conditions of LSCO and BFO films grown on silicon wafer by PLD method.

The oxygen pressure in the chamber during the deposition of the polycrystalline BFO films is 3 Pa. the temperature of the substrate is kept at 700°C. Details about the deposition conditions of BFO films are also listed in table 1. The deposition of BFO films is carried out for 90 minutes. After the deposition, the BFO films are cooled to 495°C slowly and held for 30 min in a certain oxygen pressure. In order to study the effect of oxygen vacancies, two kinds of BFO films are fabricated by PLD. For the BFO film containing less vacancy of oxygen, the oxygen pressure in the chamber is 1.01×10^5 Pa when the sample is held at 495°C for 30min. For the sample containing more vacancy of oxygen, the oxygen pressure in the chamber is just 3 Pa when the sample is kept at 495°C for 30min (Li, 2008).

2.2 The fabrications of BFO films by CSD method

Regarding the preparation of polycrystalline BFO films by CSD method, single crystal STO is used as substrate. A layer of LNO is fabricated on the surface of STO before the preparation of BFO films. The layer of LNO is also fabricated by CSD method and is used as bottom electrode. Both STO and LNO are perovskite structure and smaller crystal constant than BFO. Therefore, the substrate and the LNO layer can induce the growth of BFO films. The fabrication of LNO layer by CSD method is same to the way has been reported in literature (Meng, 2001). For the synthesizing of LNO precursor, lanthanum nitrate and nickel acetate are used as starting materials. The mixture of acetic acid and water are used as solvent. Lanthanum nitrate and nickel acetate with a stoichiometric molar ratio of 1:1 are dissolved in the solvent. The concentration of the precursor is 0.3mol/L. For the preparation of the LNO layer, the LNO precursor is spin-coated on STO substrate at 3000rpm for 20 s. the wet film is dried at 180^{o}C for 300s in a rapid thermal process furnace. Then the dried film is calcined at 380^{o}C for 300s for the organic compound pyrolyzing. Finally, the amorphous film is annealed at 650^{o}C for 300s for crystallization. The cycle of coating and thermal process are repeated six times to obtain LNO layer with expected thickness.

In regard to the synthesizing of BFO precursor, bismuth nitrate and nickel acetate are used as starting materials. Acetic acid is used as solvent (Li, 2005). The fabrication of BFO film is also contained two steps, spin-coating precursor on LNO covered STO substrate and rapid thermal process in furnace. The precursor is spin-coated at 4000rpm for 20 s. The film is dried at 180^{o}C for 240s, pyrolyzed at 350^{o}C for 240s, and annealed at 600^{o}C for 240s. Two kinds of BFO films with different electrical resistivity are fabricated.

2.3 The crystalline and electrical characterizations

The crystallinity of BFO, LSCO, and LNO films is characterized by x-ray diffraction (XRD) using Cu Kα as radiation source (D/MAX-2550V, Rigaku Co.). During the XRD measurement, the continuous θ-2θ scanning mode with the interval of 0.02^o is used. All XRD characterizations are carried out at room temperature. For the electrical measurement, platinum is used as top electrode. Platinum dots with the diameter of 2×10^{-2}cm are sputtered onto the surface of the polycrystalline BFO films using a shadow mask. The ferroelectric properties are measured using a ferroelectric test system (Permier II, Radiant Technologies, Inc.). During the measurement, the frequency of the alternating current (ac) signal is 1 kHz. Two triangle waves with different polarity are used as the applied voltage. Before each measurement of hysteresis loop, a pre-polar voltage is applied on the film. The dielectric properties of the polycrystalline BFO films are measured using an impedance analyzer (Hewlett-Packard 4194A). The voltage of the small ac signal is 0.05V. The frequency dependence of the permittivity and dielectric loss is measured in the frequency range from 100 Hz to 1 MHz. The voltage dependence of the permittivity is measured at 1 MHz. The leakage current behaviour of the polycrystalline BFO films under dc voltage bias is measured using an electrometer (Keithley 6517A). Besides the electrical measurements carried out at room temperature, the temperature dependence permittivity and leakage current measurements are carried out at different temperatue and the temperature is controlled with an accuracy of ±0.5K using a variable temperature micro-probe stage (K-20, MMR technologies, Inc.).

3. Crystalline structures

Because the impurity has great effects on the electrical properties of the BFO films, it is important that the studied polycrystalline BFO films do not contain any impurity or parasitical phase. The structure of the polycrystalline BFO films fabricated by PLD and CSD on different substrates is investigated firstly.

3.1 The crystalline structure of BFO films fabricated by PLD method

Figure 1 shows the XRD curves of the polycrystalline BFO films grown on LSCO covered silicon substrate and thermal treated at different oxygen pressure. The XRD curve of LSCO film grown on silicon wafer by PLD method is also exhibited in the figure. The indexes of each diffractive peak are labelled in the figure. The indexes of pseudo-cubic structure are used for BFO films.

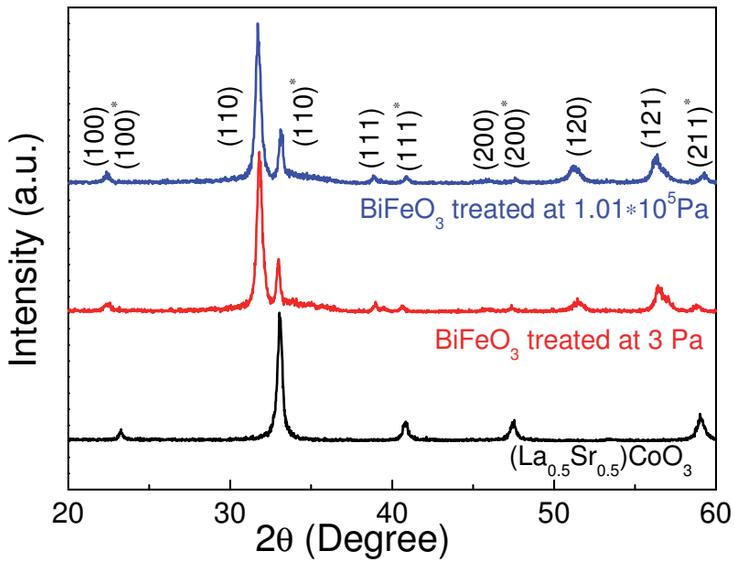

Fig. 1. The XRD patterns of $(La_{0.5}Sr_{0.5})CoO_3$ film and $BiFeO_3$ films fabricated by PLD method and thermal treated at different oxygen pressure. The labels contained a star (*) indicate the diffractive peaks of LSCO. The indexes of pseudo-cubic structure are used to label the diffractive peaks of BFO films.

There is no any trace of impure phase in the XRD curves of the polycrystalline BFO films thermal treated at 1.01×10^5 Pa or 3 Pa. Neither LSCO nor BFO films exhibit (100) preferential orientation even the (100) silicon wafer is used as substrate. The position of the diffractive peak does not show perceptible shift for the two kinds of BFO films thermal treated at different oxygen pressure. It indicates that the thermal process at different oxygen pressure does not affect the crystalline structure of the polycrystalline BFO films. The pseudo-cubic crystal constant calculated from the XRD curve is about 3.96Å. This value is close to the value of bulk BFO (JCPDS: 74-2016). Therefore, even the crystal constant of LSCO is smaller than that of BFO, the mismatch between BFO and LSCO has no effect on the crystalline structure of the polycrystalline BFO films. Moreover, the full width at half maximum (FWHM) of the diffractive peak has no obvious variety. It indicates that the size of the crystal grain in the two kinds of BFO films is not influenced by the difference of the thermal process.

3.2 The crystalline structure of BFO films fabricated by PLD method

Figure 2 shows the XRD curve of polycrystalline BFO film grown on LNO covered (100)STO substrate. The position and relative intensity of the diffractive peak for bulk BFO is also exhibited in the figure. The data of the bulk BFO comes from JCPDS and is used to discuss the difference between the polycrystalline film and bulk.

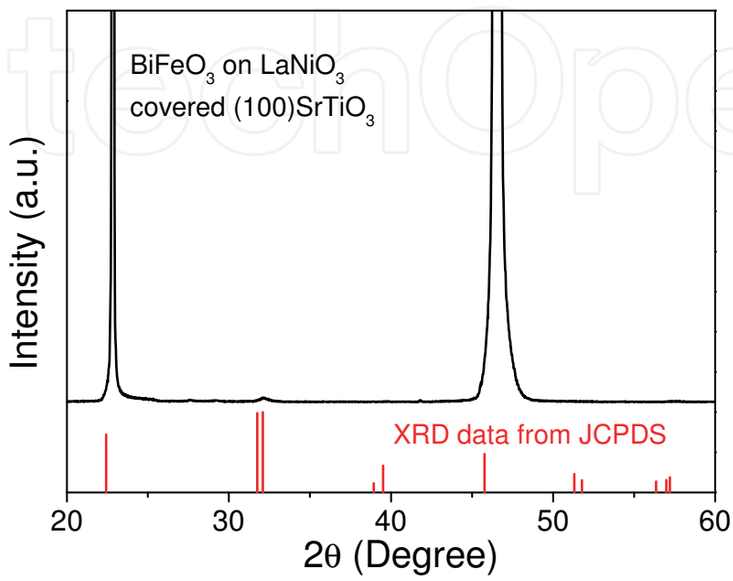

Fig. 2. The XRD patterns of $BiFeO_3$ films grown on $LaNiO_3$ covered (100)$SrTiO_3$ substrate by chemical solution deposition. The data of bulk $BiFeO_3$ (JCPDS: 74-2016) is also displayed in this figure using short straight line. The height of the straight line represents the relative intensity of the diffractive peak.

Compared with the BFO films grown on LSCO covered (100) silicon substrate by PLD method, the BFO film grown on LNO covered (100) STO substrate exhibits highly (100) preferential orientation. It can be ascribed to the inducement from the substrate with perovskite structure and smaller mismatch between BFO, LNO and STO. The existence of (110) and (104) diffractive peaks indicate that the BFO film is not epitaxial monocrystalline film but polycrystalline film. Compared with the XRD data of BFO bulk, the diffractive peaks shift towards higher angle. This means that the out-of-plane crystal constant of the BFO film is smaller than that of BFO bulk.

4. Electrical properties of polycrystalline BFO films

Ferroelectric hysteresis, dielectric response and leakage behaviour are the primary electrical characterization of ferroelectric films. Most of these electrical performances are related to the temperature. In this section, the electrical properties of polycrystalline BFO films fabricated by different methods are studied at different temperature.

4.1 Dielectric response of polycrystalline BFO films

The frequency dependence of capacitance and loss tangent of polycrystalline BFO films fabricated by PLD and CSD methods are shown in figure 3 and figure 4, respectively.

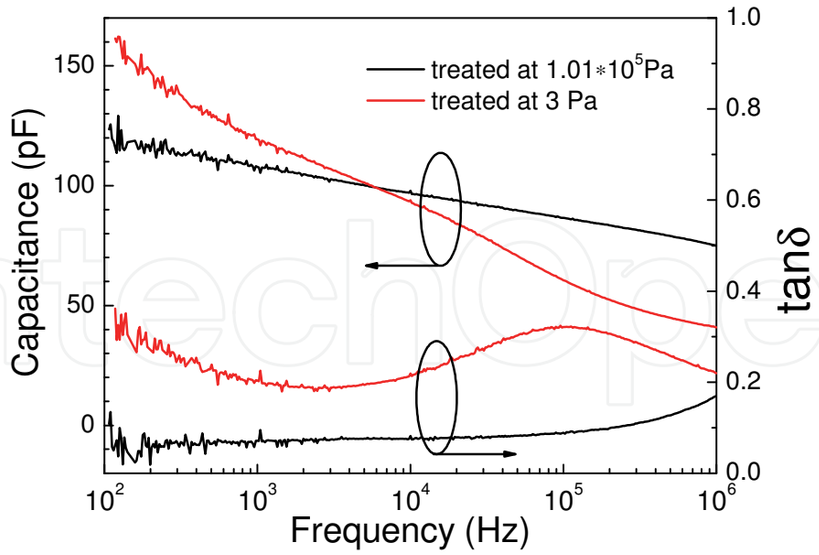

Fig. 3. The frequency dependence of capacitance and loss tangent of BFO films prepared by PLD method and thermal treated at 1.01×10^5 Pa (black) or 3 Pa (red).

The capacitance of BFO film treated at 1.01×10^5 Pa decreases approximatively linearly with the frequency increasing. The value of loss tangent keeps about 0.08 at the frequency range between 100 Hz and 100 kHz, and rises to about 0.17 when the frequency achieves to 1 MHz. the capacitance of the BFO film treated at 3 Pa decreases faster than that of the film treated at 1.01×10^5 Pa. The loss tangent of the film treated at 3 Pa is larger than that of the film treated at 1.01×10^5 Pa. The loss tangent increases with the frequency decreasing in the frequency range between 100 Hz and 1 kHz. The increase of loss tangent at lower frequency range suggests that the dc leakage current is higher in this BFO film. In addition, there is a broad relaxation peak near 10^5 Hz in the loss tangent curve.

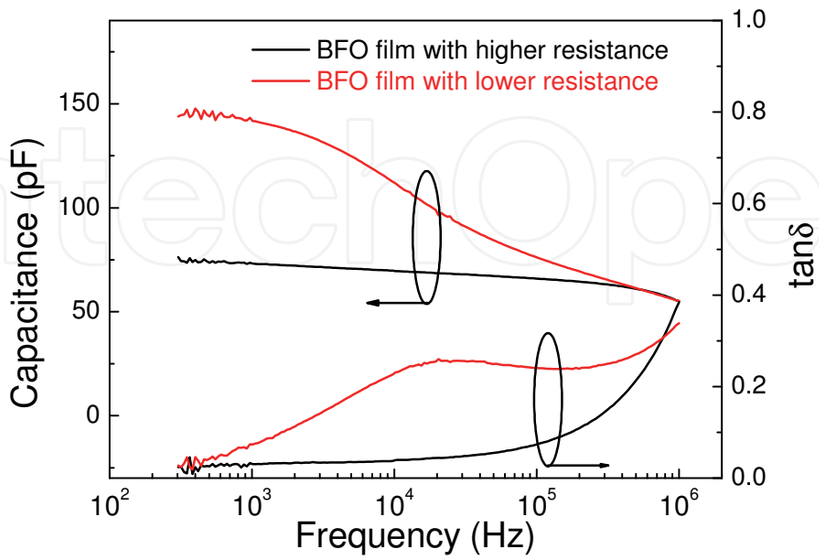

Fig. 4. The frequency dependence of capacitance and loss tangent of BFO films prepared by CSD method.

Similar phenomena can be observed from the frequency dependence of capacitance and loss tangent of BFO films fabricated by CSD method, as shown in fig. 4. The frequency dependence of capacitance and loss tangent of BFO film with higher resistivity is similar to the results of the BFO film prepared by PLD method and thermal treated at 1.01×10^5 Pa. The capacitance of the BFO film with lower resistivity decreases faster than that of the BFO films with higher resistivity, and an obvious relaxation peak can be observed from the frequency dependence of loss tangent. Similar results have also been reported in pure and lanthanum-substituted BFO film (Singh et al., 2007). According to Singh's result, the leakage current in BFO films can be depressed greatly by substituting part bismuth using lanthanum. The frequency dependence of relative dielectric constant of pure BFO film varies distinctly compared with that of the lanthanum-substituted BFO film. A broad relaxation peak exists in the frequency dependence of loss tangent of the pure BFO film but can not be observed in the frequency dependence of loss tangent of the lanthanum-substituted BFO film. All of these results suggest that the evident variety of permittivity and the broad relaxation peak in the frequency dependence of loss tangent are relative to the higher leakage current in the polycrystalline BFO films. Because that the BFO films fabricated by PLD method and thermal treated at different oxygen pressure, the density of the vacancy of oxygen is different. The results of BFO films fabricated by PLD method also confirm that the dielectric relaxation in the BFO films with lower electrical resistivity is relevant to the defect of oxygen.

Dielectric relaxation process related to the vacancy of oxygen usually follows the Debye-type law. This kind of process can be represented by the empirical expression established by Cole and Cole (Cole & Cole, 1941)

$$\varepsilon^*_{cole} = \varepsilon_\infty + \frac{\varepsilon_s - \varepsilon_\infty}{1+(i\omega\tau)^{1-\alpha}} \tag{1}$$

Where ε^*_{cole} is the complex dielectric constant, ε_s is the static dielectric constant, ε_∞ is the dielectric constant at high frequency, τ is relaxation time and ω is the circular frequency. α is a parameter which is used to describe the distribution of relaxation time. The value of α is between 0 and 1. When α equals to 0, the equation (1) is simplified to Debye model, which has a certain relaxation. Besides the dielectric relaxation related to oxygen vacancies, there are some other factors which have contributions to the dielectric response in the polycrystalline BFO films with lower electrical resistivity. These factors exist also in the BFO films with higher electrical resistivity. The dielectric response of these factors does not display the Debye-type relaxation and can be represented by universal dielectric response (UDR) model. In this model, the real part and imaginary part of complex dielectric constant can be described respectively as (Lunkenhjeimer et al.,2002; Tselev et al., 2004)

$$\begin{aligned} \varepsilon_{rT} &= \frac{1}{\varepsilon_0}\sigma_0 \tan\left(\frac{\pi}{2}s\right)\omega^{s-1} \\ \varepsilon''_T &= \frac{\sigma_{dc}}{\omega\varepsilon_0} + \frac{\sigma_0}{\varepsilon_0}\omega^{s-1} \end{aligned} \tag{2}$$

where ε_{rT} and ε''_T are the real part and imaginary part of complex dielectric constant. σ_{dc} is the dc electric conductivity, which is induced by the leakage current. σ_0 is a pre-power term

and *s* is a parameter with the value between 0 and 1. Considering the dielectric response related to the oxygen vacancies and all the other dielectric response processes, the frequency dependence of complex dielectric constant of the BFO films with lower electrical resistivity should following a model which is constituted by Cole-Cole's model and UDR model. The expression of the model is

$$\varepsilon^* = \varepsilon^*_{cole} + \varepsilon^*_T \tag{3}$$

where ε^* is the complex dielectric constant of polycrystalline BFO films with lower electrical resistivity, ε^*_{cole} and ε^*_T are the complex dielectric constant contributed by the relaxation processes related to oxygen vacancies and the dielectric response process following UDR model respectively. For the polycrystalline BFO film fabricated by PLD method and thermal treated at 3 Pa, the measured circular frequency dependence of complex dielectric constant and fitting results according to equation (3) is shown in fig. 5 (Li, 2008). The values of some parameters in the model are listed in table 2.

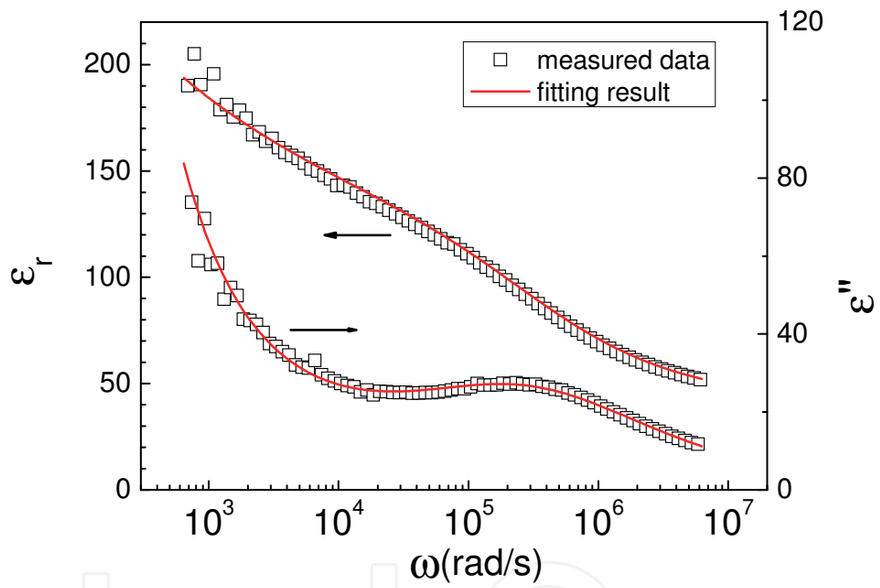

Fig. 5. The measured circular frequency dependence of complex dielectric constant and the fitting results for the polycrystalline BFO films fabricated by PLD method and thermal treated at 3 Pa.

According to the fitting results, the electrical resistivity of the polycrystalline BFO film fabricated by PLD and thermal treated at 3 Pa is less than the orders of magnitude $10^9\Omega\cdot$cm. This result coincides with the published work (Eerenstein, 2005). The lower electrical resistivity means higher leakage current in the films, which obstructs the measurement of ferroelectric properties of polycrystalline BFO films.

τ (s)	σ_{dc} ($\Omega^{-1}\cdot cm^{-1}$)	σ_0 ($\Omega^{-1}\cdot cm^{-1}$)	α	s
3.35×10^{-6}	2.61×10^{-9}	2.02×10^{-11}	0.60	0.72

Table 2. Values of some parameters used in the Debye and UDR combinatorial model.

Besides the relaxation process related to defect of oxygen, the interfacial polarization which occurs between the ferroelectric film and the electrode has significant impact on the measured dielectric response. Liu *et al.* have reported their results on the interfacial polarization between BFO films and the electrode (Liu, 2008). If there is the dielectric response induced by the interfacial polarization, the measured frequency dependence of capacitance will change significantly when different dc bias voltage applied on the samples (Zhang, 2005; Liu, 2008). The frequency dependence of capacitance of the polycrystalline BFO film fabricated by PLD and thermal treated at 3 Pa is measured under dc bias voltage between 0 and 3V. The results are shown in Fig. 6. In contrast to the results reported by Liu *et al.* (Liu, 2008), the curves of the frequency dependence of capacitance measured under different dc bias voltage almost overlap for our sample. A small difference between the curves can be observed from the enlarged plot. The difference dues to the nature of ferroelectrics that dielectric constant changes with the applied dc voltage. It is indicated that the dielectric response contributed by interfacial polarization between the BFO film and electrode can be ignored in our sample.

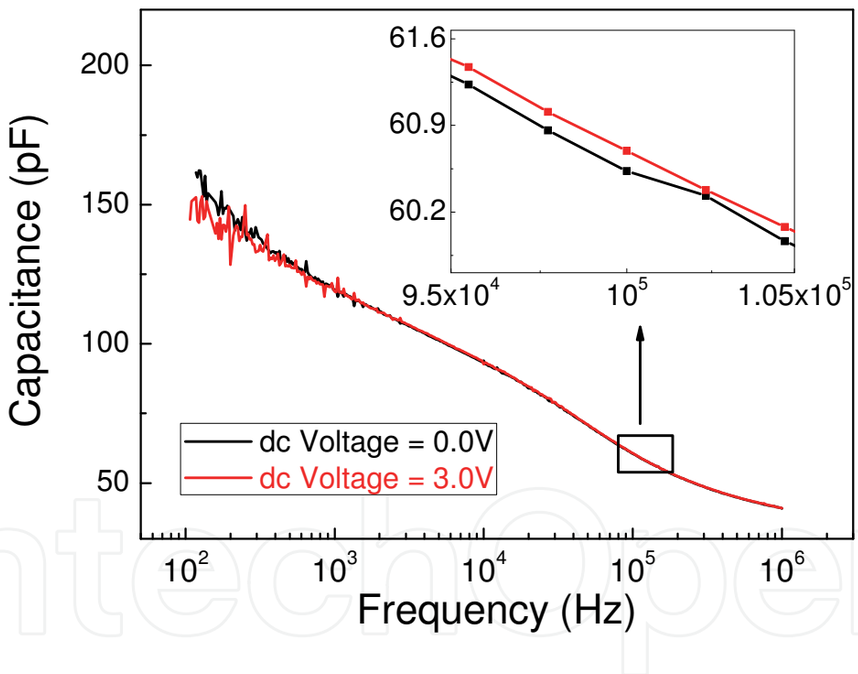

Fig. 6. The frequency dependence of capacitance of the polycrystalline BFO films fabricated by PLD method and thermal treated at 3 Pa measured at different dc bias voltage (0V and 3V). The inset figure exhibits the enlarged parts of the curves nearby 100 kHz.

Now, it is confirmed that the Debye-type relaxation process in polycrystalline BFO films with lower electrical resistivity is related to oxygen vacancies. More research is needed to investigate how the oxygen vacancies work. The dielectric relaxation process related to oxygen defects in the polycrystalline BFO films fabricated by CSD method with lower electrical resistivity is studied at different temperature.

Figure 7 display the temperature dependence of capacitance and loss tangent of polycrystalline BFO film with lower electric resistivity prepared by CSD method in the temperature range between 230K and 430K. The results are measured at different frequency. The capacitance decreases with the increase of the measuring frequency at a certain temperature. This result is consistent with the frequency dependence of capacitance of polycrystalline BFO films prepared by PLD method. A broad peak can be observed in the temperature dependence of loss tangent. The peak position shifts to higher temperature with the increase of the measuring frequency.

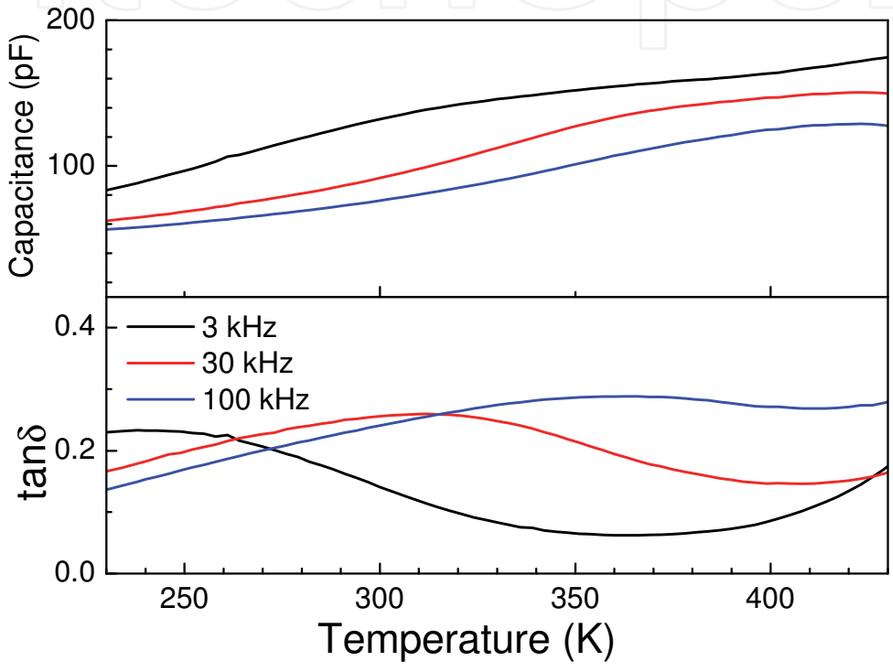

Fig. 7. The temperature dependence of capacitance and loss tangent of the polycrystalline BFO films fabricated by CSD method.

The temperature corresponds to the maximum of loss tangent at a certain measuring frequency is denoted as T_m. The value of T_m increases with the increase of the measuring frequency. The relationship between the logarithm of frequency and the reciprocal of T_m is plotted in Fig. 8 Inset. The relationship between the logarithm of measuring frequency and the reciprocal of T_m is nearly linear. It is suggested that the relationship between the measuring frequency and T_m following the Arrehenius law, which can be expressed as (Samara, 2003)

$$f = f_0 \exp\left(-\frac{E}{k_B T_m}\right) \tag{4}$$

Where f_0 is the pre-exponential term and E is the activation energy for the relaxation process, k_B is the Boltzmann's constant.

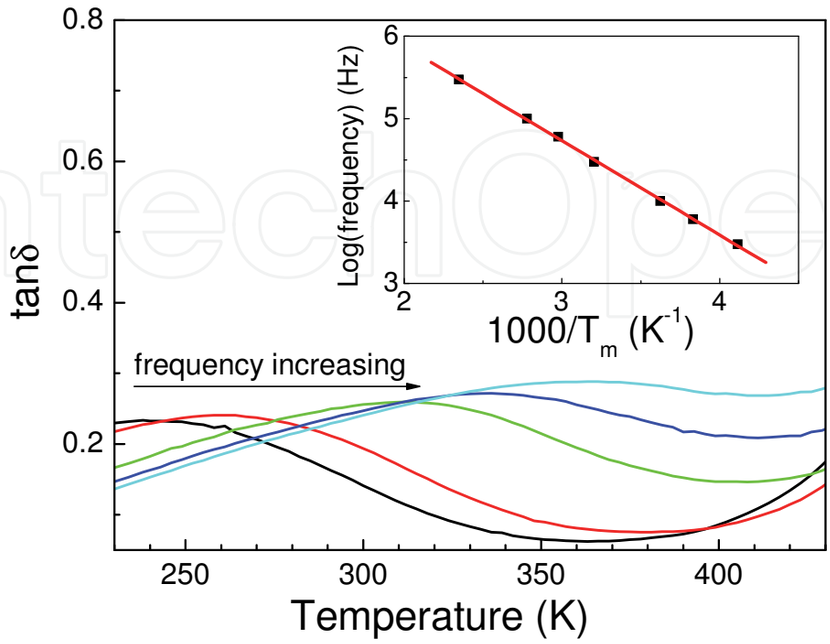

Fig. 8. The temperature dependence of loss tangent of the polycrystalline BFO films fabricated by CSD method. The value of T_m increases with increase of the measuring frequency. The Inset displays the relationship between the measuring frequency and the reciprocal of T_m. The straight line is linear fitting for the experimental data.

According to the result of linear fitting, the activation energy for the relaxation process related to oxygen vacancies is about 230 meV. As reported, the activation energy for dipolar relaxation in ferroelectrics is about 100~400meV (Samara, 2003). Therefore, the relaxation process with the activation energy of 230 meV in our samples may be a kind of dipolar relaxation process related to oxygen vacancies. Besides the vacancy of oxygen, another primary defect is Fe^{2+} (Palkar, 2002; Yun, 2003; Y. P. Wang, 2004). Therefore, it is suggested that the dipolar which induced this relaxation process is composed by vacancy of oxygen and Fe^{2+} (Vo-Fe^{2+}). It should be pointed out that the transfer of polaron in ferroelectrics also has the dielectric response similar to what has been observed above. But the activation energy for transfer of polaron is lower than the value calculated from our samples in the order of magnitude (Bidault, 1995). Therefore, the possible contribution from the transfer of polaron is excluded.

4.2 Ferroelectric and leakage behaviors of polycrystalline BFO films

As mentioned above, the higher leakage current in polycrystalline BFO films is related to the presence of a large number of oxygen vacancies. For the BFO film with higher electrical resistivity prepared by CSD method, the ferroelectric properties can be measured at lower temperature. The hysteresis loops and voltage dependence of capacitance of the sample measured at 70K are shown in Fig. 9.

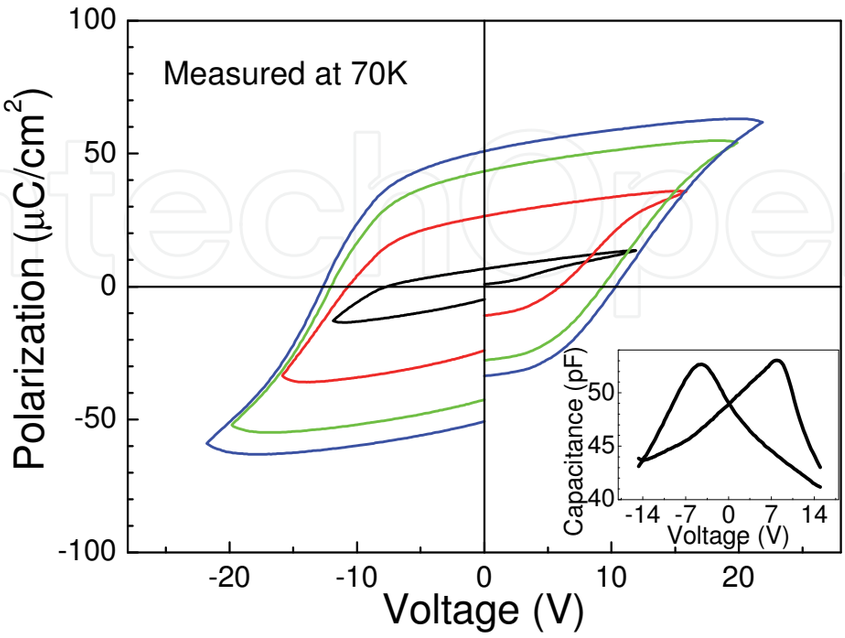

Fig. 9. The hysteresis loops under different applied voltages for the polycrystalline BFO film fabricated by CSD method. The inset displays the voltage dependence of the capacitance. Both ferroelectric hysteresis and the voltage dependence of the capacitance are measured at 70 K.

As shown in Fig. 9, the hysteresis loop exhibits the trend of saturation when the applied voltage is higher than 16V. The difference between the sample under positive bias and negative bias may be induced by the different top and bottom electrodes. Correspondingly, the voltage dependence of capacitance also shows an asymmetric butterfly-shape curve. According to the definition (Park, 2000)

$$tunability = (C_{\max} - C_{\min}) / C_{\max} \tag{5}$$

where C_{max} and C_{min} are the maximum and minimum of the capacitance under different applied voltage, the tunability of capacitance for the polycrystalline BFO film prepared by CSD method is about 22% at 70K.

However, when the temperature increases, the leakage current rises rapidly. The leakage current is so high that the film is breakdown before saturation under an applied voltage at room temperature. The measurements on the ferroelectric properties are impossible for this BFO film. Therefore, it is useful to study the leakage behaviour and the relationship between the leakage current and temperature.

The conductance of the polycrystalline BFO film prepared by CSD method is measured under different voltage at the temperature range between 80K and 350K. The results are exhibited in Fig. 10 (Sun, 2006).

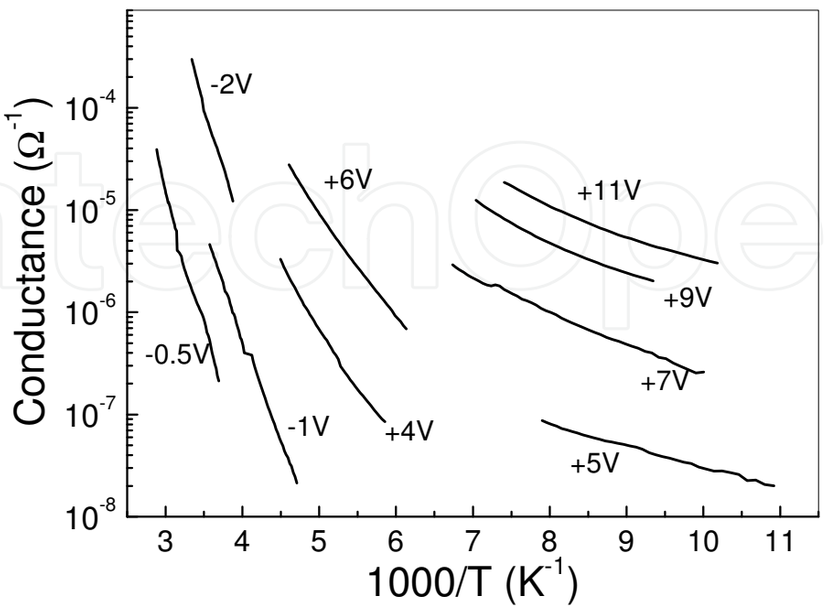

Fig. 10. The temperature dependence of conductance under different applied voltage of BFO film prepared by CSD method. The labels nearby each lines is the voltage applied on the film. (Sun, 2006)

In the semi-log plot, the relationship between the conductance and the reciprocal of temperature is approximately linear. This relationship follows the Poole-Frenkel (PF) emission (Pabst, 2007; Yang, 2008), which can be expressed as

$$\sigma_{PF} = c\exp\left[-\frac{1}{k_B T}\left(E_I - \sqrt{\frac{q^3 V}{\pi\varepsilon_0\varepsilon_r d}}\right)\right] \tag{6}$$

where c is a constant and E_I is the trap ionization energy which is related to the hopping of charge carrier. V is the voltage applied on the BFO film and d is the thickness of the BFO film. According to Pabst's report, the PF emission is the dominant transport mechanism in epitaxial BFO films (Pabst, 2007). Therefore, it is reasonable that PF emission is also one of the dominant leakage mechanisms in polycrystalline BFO film. However, there is an obvious difference between the experimental results of epitaxial and polycrystalline films. For epitaxial BFO films, the slope of the line *log(σ)* vs. *1000/T* varies linearly with the applied voltage (Pabst, 2007). But the slope of the lines in Fig. 10 has great difference. The lines can be divided into two groups according to their slope. According to equation (6), the relationship between the slope and the square root of the applied voltage can be expressed as

$$slope = \frac{1}{k_B}\sqrt{\frac{q^3 V}{\pi\varepsilon_0\varepsilon_r d}} - \frac{1}{k_B}E_I = c'\sqrt{V} - \frac{E_I}{k_B} \tag{7}$$

The coefficient c' is related to the dielectric constant ε_r. Regarding the data measured under higher applied voltage, the result is close to the epitaxial BFO film. However, for the data measured under lower applied voltage, the derived dielectric constant is one order of magnitude smaller than the reported value. In order to study the origin of the difference under different voltages, conductive tip atomic force microscopy (CAFM) is used.

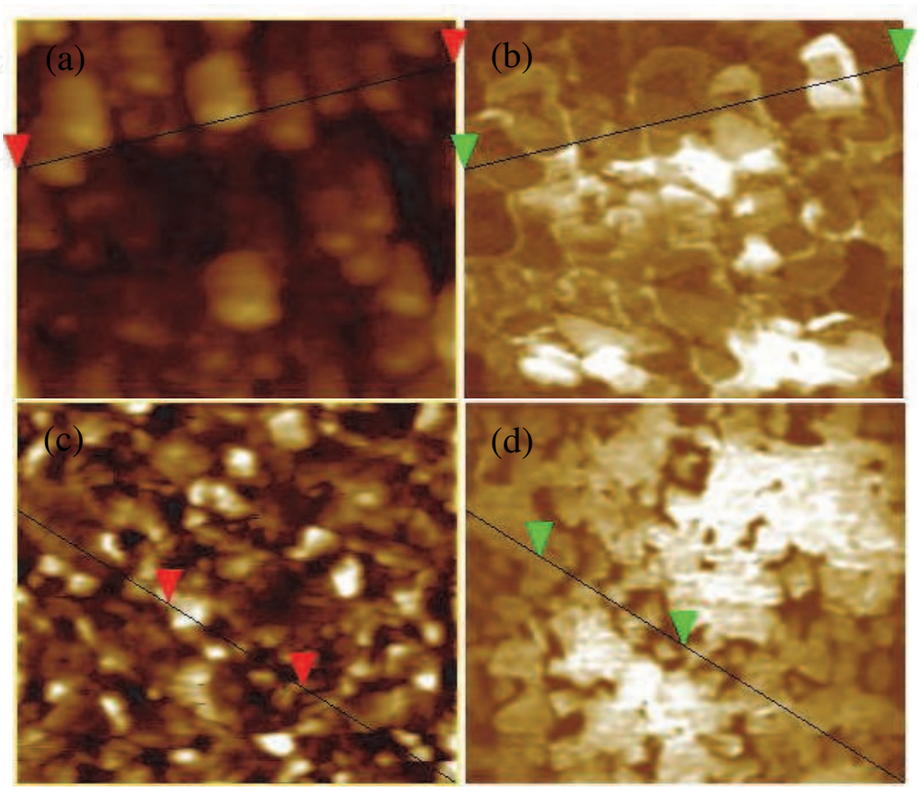

Fig. 10. The images of conductive tip atomic force microscopy (Area 1μm×1μm). (a) Surface morphology of the BFO film under 2.5 V voltage; (b) Current mapping of the BFO film under 2.5V voltage; (c) Surface morphology of the BFO film under 4.5 V voltage; (d) Current mapping of the BFO film under 4.5V voltage (Sun, 2006).

Figure 10 displays the CAFM images with different voltages applied on the tip. When the applied voltage is 2.5V, the area of grain boundary is highlight in fig. 10(b). This means that the leakage current flows along the grain boundary. When the applied voltage rises to 4.5V, all the grain is highlight. This means the current flows primarily through the whole grains. Comparing to the results of the leakage measurements, it is inferred that there is a region with lower dielectric constant at the grain boundary area. This region is the transfer access for leakage current when the voltage applied on the samples is smaller (Sun, 2006).

4.3 Ferroelectrics of polycrystalline BFO films on buffered silicon wafer

Compared to the BFO films grown on STO substrate, BFO films grown on silicon wafer has broader application prospects once the leakage problem is resolved. Figure 11 exhibits the ferroelectric hysteresis of the polycrystalline BFO films grown on LNO buffer silicon wafer.

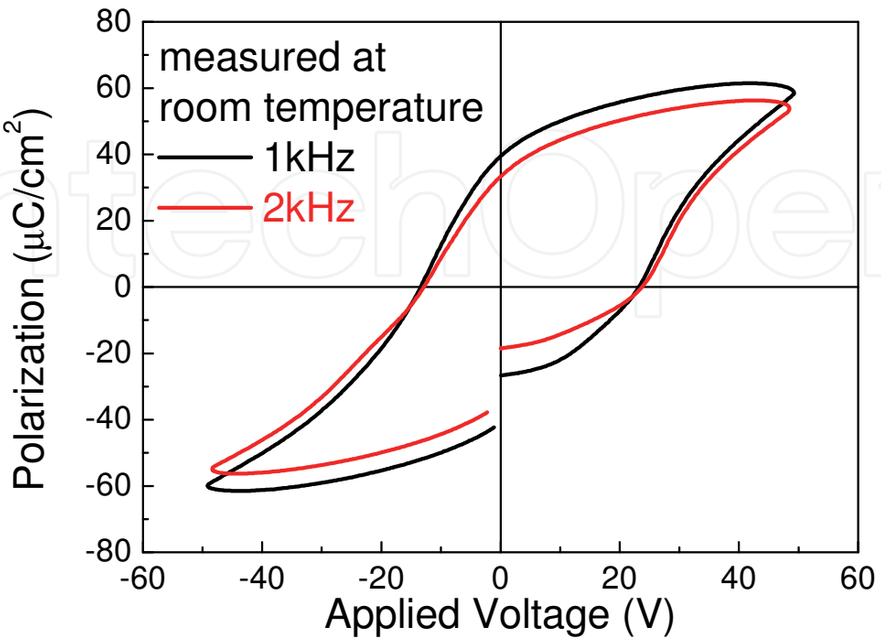

Fig. 11. The ferroelectric hysteresis of the polycrystalline BFO films grown on LNO buffer silicon wafer.

The layer of BFO is grown by PLD method and the buffer layer/bottom electrode LNO is fabricated by CSD method. The measurements are carried out at room temperature. Compared to the LSCO buffer layer fabricated by PLD, LNO layer fabricated by CSD is a more suitable buffer layer for the growth of high quality polycrystalline BFO films. Compared to the epitaxial BFO films on buffered-STO substrate, the value of Pr of polycrystalline BFO films is smaller. But the value is still larger than that of PZT and BTO films. Therefore, it is useful for the substitution of PZT in FeRAM.

5. Conclusion

In summary, the polycrystalline BFO films are fabricated on buffered silicon wafer and STO substrates. The electrical processes in the polycrystalline BFO films are investigated. The existence of a large number of oxygen vacancies not only increases the leakage current in BFO films, but also influence the dielectric response of the polycrystalline BFO films. The dielectric response is contributed in the form of dipolar combined by oxygen vacancy and Fe^{2+}. For the polycrystalline BFO films do not contain many oxygen vacancies, the Poole-Frenkel emission is the dominant transport mechanism when the polycrystalline BFO film. A region with lower dielectric constant exists at the grain boundary in polycrystalline BFO films. This region is the primary leakage access when the polycrystalline BFO film is under lower applied voltage. These results have significance for the researches on the applications of film in microelectronic devices.

6. Acknowledgments

One of the authors (Y. W. Li) thanks Prof. J. L. Sun for the useful discussion. This work was financially supported by Natural Science Foundation of China (Grant Nos. 60906046 and 11074076), Major State Basic Research Development Program of China (Grant Nos. 2007CB924901 and 2011CB922200), Projects of Science and Technology Commission of Shanghai Municipality (Grant Nos. 10DJ1400201, 10SG28, 10ZR1409800, and 09ZZ42), the Innovation Research Project of East China Normal University, and the Program for Professor of Special Appointment (Eastern Scholar) at Shanghai Institutions of Higher Learning.

7. References

Bidault O. ; Maglione M. ; Actis M. ; Kchikech M. (1995). Polaronic relaxation in perovskites. *Phys. Rev. B* 52, 4191. ISSN : 0163-1829.

Cole K. S. ; Cole R. H. (1941). Dispersion and absorption in dielectrics. *J. Chem. Phys.*, 9, 341. ISSN : 0021-9606.

Eerenstein W. ; Morrison F. D. ; Dho J. ; Blamire M. G. ; Scott J. F. ; Mathur N. D. (2005). Comment on "Epitaxial $BiFeO_3$ multiferroic thin film heterostructures". *Science*, 307, 1203a. ISSN : 0036-8075.

Hauser A. J. ; Zhang J. ; Mier L. ; Ricciardo R. A. ; Woodward P. M. ; Gustafson T. L. ; Brillson L. J. ; Yang F. Y. (2008). Characterization of electronic structure and defect states of thin epitaxial $BiFeO_3$ films by UV-visible absorption and cathodoluminescence spectroscopies. *Appl. Phys. Lett.*, 92, 222901. ISSN : 0003-6951.

Kaczmarek W., Pajak Z. & Polomska M.(1975). Differential thermal analysis of phase transitions in $(Bi_{1-x}La_x)FeO_3$ solid solution. *Solid. State. Comm.*, 17, 807. ISSN : 0038-1098.

Li Y. W. ; Sun J. L. ; Chen J. ; Meng X. J. ; Chu J. H. (2005). Preparation and characterization of $BiFeO_3$ thin films grown on $LaNiO_3$-coated $SrTiO_3$ substrate by chemical solution deposition. *J. Cryst. Growth*, 285, 595. ISSN : 0022-0248.

Li Y. W. ; Hu Z. G. ; Yue F. Y. ; Yang P. X. ; Qian Y. N. ; Cheng W. J. ; Ma X. M. ; Chu J. H. (2008). Oxygen-vacancy-related dielectric relaxation in $BiFeO_3$ films grown by pulsed laser deposition. *J. Phys. D : Appl. Phys.*, 41, 215403. ISSN : 0022-3727.

Li Y. W. ; Hu Z. G. ; Yue F. Y. ; Zhou W. Z. ; Yang P. X. ; Chu J. H. (2009). Effects of deposition temperature and post-annealing on structure and electrical properites in $(La_{0.5}Sr_{0.5})CoO_3$ films grown on silicon substrate. *Appl. Phys. A*, 95, 721. ISSN : 0947-8396.

Liu G. Z. ; Wang C. ; Wang C. C. ; Qiu J . ; He M. ; Xing J. ; Jin K. J. ; Lu H. B. ; Yang G. Z. (2008). Effects of interfical polarization on the dielectric properties of $BiFeO_3$ thin film capacitors. *Appl. Phys. Lett.*, 92,122903. ISSN : 0003-6951.

Lunkenheimer P. ; Bobnar V. ; Pronin A. V. ; Ritus A. I. ; Volkov A. A. ; Loidl A. (2002). Origin of apparent colossal dielectric constants. *Phys. Rev. B* 66, 052105. ISSN : 0163-1829.

Maruyama K. ; Kondo M. ; Singh S. K. ; Ishiwara H. (2007). New ferroelectric material for enbedded FRAM LSIs. *FUJITSU Sci. Tech. J.* , 43, 502. ISSN : 0016-2523.

Meng X. J. ; Sun J. L. ; Yu J. ; Ye H. J. ; Guo S. L. ; Chu J. H. (2001). Preparation of highly (100)-oriented metallic $LaNiO_3$ films on Si substrates by a modified metalorganic decomposition technique. *Appl. Surf. Sci.*, 171, 68. ISSN : 0169-4332.

Pabst G. W. ; Martin L. W. ; Chu Y. H . ; Ramesh. R. (2007). Leakage mechanisms in $BiFeO_3$. *Appl. Phys. Lett.*, 90, 072902. ISSN : 0003-6951.

Palkar V. R. ; John J. ; Pinto R. (2002). Observation of saturated polarization and dielectric anomaly in magnetoelectric $BiFeO_3$ thin films. *Appl. Phys. Lett.*, 80, 1628. ISSN : 0003-6951.

Park B. H. ; Gim Y. ; Fan Y . ; Jia Q. X. ; Lu P. (2000). High nonlinearity of $Ba_{0.6}Sr_{0.4}TiO_3$ films heteroepitaxially grown on MgO substrates. *Appl. Phys. Lett.*, 77, 2587. ISSN : 0003-6951.

Samara G. A. (2003). The relaxational properties of compositionally disordered ABO_3 perovskites. *J. Phys : Condens. Matter*, 15, R367. ISSN : 0953-8984.

Singh S. K. ; Maruyama K. ; Ishiwara H. (2007). The influence of La-substitution on the micro-structure and ferroelectric properties of chemical-solution-deposited $BiFeO_3$ thin films. *J. Phys. D : Appl. Phys.*, 40, 2705. ISSN : 0022-3727.

Sun J. L. ; Li Y. W. ; Li T. X. ; Lin T. ; Chen J. ; Meng X. J. ; Chu J. H. (2006). The leakage current in $BiFeO_3$ films derived by chemical solution deposition. *Ferroelectrics*, 345, 83. ISSN : 0015-0193.

Teague J. R.; Gerson R. & James W. J. (1970). Dielectric hysteresis in single crystal $BiFeO_3$. *Solid. State. Comm.*, 8, 1073. ISSN : 0038-1098.

Tselev A. ; Brooks C. M. ; Anlage S. M. ; Zheng H. M. ; Salamanca-Riba L. ; Ramesh R. ; Subramanian M. A. (2004). Evidence for power-law frequency dependence of intrinsic dielectric response in the $CaCu_3Ti_4O_{12}$. *Phys. Rev. B* 70, 144101. ISSN : 0163-1829.

Yang H. ; Wang H. Zou G. F. ; Jain M. ; Suvorova N. A. ; Feldmann D. M. ; Dowden P. C. ; DePaula R. F. ; MacManus-Driscoll J. L. ; Taylor A. J. ; Jia Q. X. (2008). Leakage mechanisms of self-assembled $(BiFeO_3)_{0.5}$:$(Sm_2O_3)_{0.5}$ nanocomposite films. *Appl. Phys. Lett.*, 93, 142904. ISSN : 0003-6951.

Wang J. ; Neaton J. B. ; Zheng H. ; Nagarajan V. ; Ogale S. B. ; Liu B. ; Viehland D. ; Vaithyanathan V. ; Schlom D. G. ; Waghmare U.V. ; Spaldin N. A. ; Rabe K. M. ; Wutting M. ; Ramesh R. (2003). Epitaxial $BiFeO_3$ multiferroic thin film heterstructures. *Science*, 299,1719. ISSN : 0036-8075.

Wang Y. P. ; Zhou L. ; Zhang M. F. ; Che X. Y. ; Liu J. M. ; Liu Z. G. (2004). Room-temperature saturated ferroelectric polarization in $BiFeO_3$ ceramics synthesized by rapid liquid phase sintering. *Appl. Phys. Lett.*, 84, 1731. ISSN : 0003-6951.

Yun K. Y. ; Noda M. ; Okuyama M. (2003). Prominent ferroelectricity of $BiFeO_3$ thin films prepared by pulsed-laser deposition. *Appl. Phys. Lett.*, 83, 3981. ISSN : 0003-6951.

Zavaliche, F. ; Shafer P. ; Ramesh R. ; Cruz M. P. ; Das R. R. ; Kim D. M. ; Eom C. B. (2005). Polarization switching in epitaxial $BiFeO_3$ films. *Appl. Phys. Lett.*, 87, 252902. ISSN : 0003-6951.

Zhang L. (2005). Electrode and grain-boundary effects on the conductivity of $CaCu_3Ti_4O_{12}$. *Appl. Phys. Lett.*, 87, 022907. ISSN : 0003-6951.

IntechOpen

IntechOpen

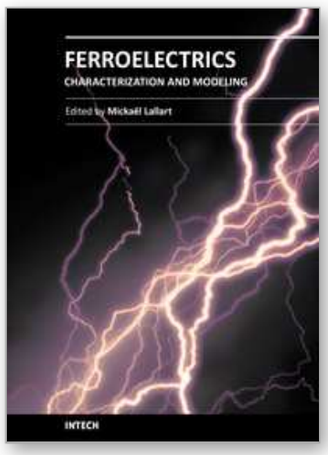

Ferroelectrics - Characterization and Modeling

Edited by Dr. MickaÃ«l Lallart

ISBN 978-953-307-455-9
Hard cover, 586 pages
Publisher InTech
Published online 23, August, 2011
Published in print edition August, 2011

Ferroelectric materials have been and still are widely used in many applications, that have moved from sonar towards breakthrough technologies such as memories or optical devices. This book is a part of a four volume collection (covering material aspects, physical effects, characterization and modeling, and applications) and focuses on the characterization of ferroelectric materials, including structural, electrical and multiphysic aspects, as well as innovative techniques for modeling and predicting the performance of these devices using phenomenological approaches and nonlinear methods. Hence, the aim of this book is to provide an up-to-date review of recent scientific findings and recent advances in the field of ferroelectric system characterization and modeling, allowing a deep understanding of ferroelectricity.

How to reference

In order to correctly reference this scholarly work, feel free to copy and paste the following:

Yawei Li, Zhigao Hu and Junhao Chu (2011). Electrical Processes in Polycrystalline BiFeO3 Film, Ferroelectrics - Characterization and Modeling, Dr. MickaÃ«l Lallart (Ed.), ISBN: 978-953-307-455-9, InTech, Available from: http://www.intechopen.com/books/ferroelectrics-characterization-and-modeling/electrical-processes-in-polycrystalline-bifeo3-film

INTECH
open science | open minds

InTech Europe
University Campus STeP Ri
Slavka Krautzeka 83/A
51000 Rijeka, Croatia
Phone: +385 (51) 770 447
Fax: +385 (51) 686 166
www.intechopen.com

InTech China
Unit 405, Office Block, Hotel Equatorial Shanghai
No.65, Yan An Road (West), Shanghai, 200040, China
中国上海市延安西路65号上海国际贵都大饭店办公楼405单元
Phone: +86-21-62489820
Fax: +86-21-62489821

© 2011 The Author(s). Licensee IntechOpen. This chapter is distributed under the terms of the Creative Commons Attribution-NonCommercial-ShareAlike-3.0 License, which permits use, distribution and reproduction for non-commercial purposes, provided the original is properly cited and derivative works building on this content are distributed under the same license.

IntechOpen

IntechOpen